Flavanols from Tetrapleura tetraptera with cytotoxic activities

Article *in* Fitoterapia · May 2022

DOI: 10.1016/j.fitote.2022.105206

9 authors, including:

Omonike Ogbole
University of Ibadan
76 PUBLICATIONS **938** CITATIONS
SEE PROFILE

Vaderament-Alexe Nchiozem-Ngnitedem
Universität Potsdam
18 PUBLICATIONS **54** CITATIONS
SEE PROFILE

Taye B. Demissie
University of Botswana
66 PUBLICATIONS **622** CITATIONS
SEE PROFILE

Mohamed Elbadawi
Johannes Gutenberg-Universität Mainz
19 PUBLICATIONS **123** CITATIONS
SEE PROFILE

Fitoterapia 160 (2022) 105206

Contents lists available at ScienceDirect

Fitoterapia

journal homepage: www.elsevier.com/locate/fitote

Flavanols from *Tetrapleura tetraptera* with cytotoxic activities

Oguntimehin Samuel Ayoolu [a,f], Omonike Oluyemisi Ogbole [a], Edith Oriabure Ajaiyeoba [a,**], Vaderament-A Nchiozem-Ngnitedem [b], Taye B. Demissie [c], Mohamed Elbadawi [d], Thomas Efferth [d], Kibrom Gebreheiwot Bedane [e,*], Michael Spiteller [f]

[a] Department of Pharmacognosy, University of Ibadan, Ibadan, Nigeria
[b] Department of Chemistry, University of Nairobi, Nairobi, Kenya
[c] Department of Chemistry, University of Botswana, Gaborone, Botswana
[d] Department of Pharmaceutical Biology, Institute of Pharmaceutical and Biomedical Sciences, Johannes Gutenberg University, Mainz, Germany
[e] Department of Chemistry, Addis Ababa University, Addis Ababa, Ethiopia
[f] Institute of Environmental Research (INFU), Department of Chemistry and Chemical Biology, TU Dortmund, Dortmund, Germany

ARTICLE INFO

Keywords:
Tetrapleura tetraptera
Fabaceae
Flavan-3-ol
Flavan-3,4-diols
Cytotoxicity

ABSTRACT

Tetrapleura tetraptera is a medicinal plant used in East and West Africa to treat inflammation and related diseases. From the stem bark of the plant, three previously undescribed flavan-3-ol derivatives named (2*R*,3*S*)-3,3′,5′,7-tetrahydroxy-4′-methoxyflavane (**1**), (2*R*,3*S*)-3′,5′,7-trihydroxy-4′-methoxyflavane-3-*O*-β-D-glucopyranoside (**2**), and (2*R*,3*S*,4*S*)-3,3′,4,5′,7-pentahydroxy-4′-methoxyflavane (**3**) were isolated with three known analogues. The structural elucidation of the compounds was performed based on NMR spectroscopy and HRMS data analyses. The absolute configurations around the stereogenic carbons were determined using Circular Dichroism (ECD) and density functional theory (DFT) calculations. The cytotoxicity of the isolated compounds was tested using resazurin reduction assay. Compound **1** was moderately active against both recalcitrant leukemia cell lines with IC_{50} values of 21.90 μM towards CCRF-CEM and 50.80 towards CEM/ADR5000. Similar level of activity was observed for compound **3** against CCRF-CEM cell line, IC_{50} = 35.50 μM. All the tested compounds were not cytotoxic compared with the standard drug, doxorubicin, with IC_{50} values of 0.0075 against CCRF-CEM and 24.30 μM against CEM/ADR5000.

1. Introduction

There is continued interest in *Tetrapleura tetraptera* due to its food and pharmacological importance. *T. tetraptera* (family Fabaceae) is an African medicinal plant well distributed in Uganda, Ghana, Tanzania, and Nigeria [1]. It is a tree of 6–30 m; smooth or rough bark; leaves with 5–7 pairs of pinnae, opposite or alternate; puberulous beneath; yellowish or pinkish flowers; and glossy dark brown fruit [2]. *Aidan* – the local name for the fruit of *T. tetraptera* among the Yoruba speaking ethnic group of Nigeria - is employed locally in the treatment of inflammations, arthritis, hypertension, microbial infections, and diabetes [1]. From the ethnopharmacology point of view, *T. tetraptera* has been reported to show hypoglycemic, anti-inflammatory, and cytotoxic activities [3,4]. Kuete and colleagues reported the cytotoxicity of the methanolic extract of *T. tetraptera* fruits against human pancreatic (MiaPaCa-2) and leukemia (CCRF-CEM and CEM/ADR5000) cancer cell lines [5]. In another study, the methanolic extract of *T. tetraptera* fruits showed anticancer activity against breast cancer subpanel and leukemia cells lines [6]. More recently, Aikins and collaborators reported the antiproliferative activity of the methanolic extract of *T. tetraptera* fruits against leukemia (Jurkat) and breast cancer (MCF-7) cell lines [7]. They further investigated the chemical composition of each extract and identified alkaloids, phenolic compounds, and terpenoids as active ingredients [7]. Recent phytochemical studies indicated the isolation of triterpene saponins of the oleanane series from its seeds and minor constituents including flavonoids and phenolic compounds [4].

All these bioactivities of the plant interested us to do phytochemical investigation. From the stem bark of this plant, we have isolated three new flavanols together with three known compounds. The cytotoxicity of the compounds was evaluated against two cancer cell lines, CCRF-

* Correspondence to: K. G. Bedane, Department of Chemistry, Addis Ababa University, P.O. Box 33658, Addis Ababa, Ethiopia.
** Correspondence to: E. O. Ajaiyeoba, Department of Pharmacognosy, University of Ibadan, Ibadan, P. O. Box, 22133, Nigeria.
E-mail addresses: edajaiye@gmail.com (E.O. Ajaiyeoba), kibrom.gebrehiwot@aau.edu.et (K.G. Bedane).

https://doi.org/10.1016/j.fitote.2022.105206
Received 19 March 2022; Received in revised form 4 May 2022; Accepted 4 May 2022
Available online 8 May 2022

CEM and CEM/ADR5000.

2. Results and discussion

The methanolic extract of the stem bark of *T. tetraptera* was subjected to absorption and size exclusion chromatography (Sephadex LH-20) followed by multistep semi-preparative HPLC to afford six compounds (**1**–**6**) (Fig. 1). The known compounds were identified as 4′-*O*-methylrobinetinidol 3′-*O*-*β*-D-glucopyranoside (**4**) [8], flemicoumarin A (**5**) [9], and reflevone (**6**) [10]. The structural elucidations of the new compounds are described below.

Compound **1** was obtained as a white amorphous paste. The HRESIMS showed a molecular ion peak at *m/z* 305.1021 $[M + H]^+$ (calcd. For $C_{16}H_{17}O_6$, 305.1019), which determined the molecular formula to be $C_{16}H_{16}O_6$. The IR spectrum disclosed absorption bands due to O-H stretching (3354 cm^{-1}) and C=C aromatic (1623 and 1458 cm^{-1}). The flavan-3-ol scaffold was evident in this compound based on signals observed in the ^{1}H NMR [(δ_H 4.66 (1H, d, J = 7.0 Hz, H-2), 4.02 (1H, td, J = 7.0, 4.9 Hz, H-3), 2.86 (1H, dd, J = 15.7, 4.9 Hz, H-4$_{eq}$), and 2.69 (1H, dd, J = 15.7, 7.6 Hz, H-4$_{ax}$))] and ^{13}C NMR [(δ_C 82.7 (C-2), 68.7 (C-3), and 32.6 (C-4))] spectra (Table 1) [9]. The aromatic proton signals δ_H 6.87 (1H, d, J = 8.2 Hz), 6.36 (1H, dd, J = 8.2, 2.4 Hz), and 6.32 (1H, d, J = 2.4 Hz) assigned to H-5, H-6, and H-8, respectively of A-ring based on coupling constants and HMBC correlations. The aromatic singlet depicted at δ_H 6.87 (2H, H-2′/6′) together with the symmetric signals observed in the ^{13}C NMR at δ_C 107.2 (C-2′/6′) and 151.7 (C-3′/5′) suggested a 3′,4′,5′-trisubstituted B-ring. In the non-aromatic region, signal of a methoxy substituent were observed at δ_H 3.81 [δ_C 60.7]. Downfield nature of this methoxy carbon compared to the normal value indicating that it was di-*ortho* substituted [11]. This allowed its position at C-4′ together with HMBC correlation of δ_H 3.81 with δ_C 136.4 (C-4′). The proton and carbon placement of B-ring was established with COSY and HMBC correlations. The COSY correlation H-2 with H-3 and H-3 with H$_2$–4 determined the connectivity sequence in the ring. In addition, HMBC correlations were observed between H-2 (δ_H 4.66) with carbons at δ_C 136.8 (C-1′) and 107.2 (C-2′/6′).

The absolute configuration was determined by coupling constants and CD data (Fig. 2). The theoretical ECD value was performed using Density Functional Theory (DFT) and Time-Dependent Density Functional Theory (TD-DFT) calculations. The calculations were performed using the B3LYP [12,13] functional together with Grimme's dispersion correction and 6–311++G** [14] basis set. The coupling constant between H-2 and H-3 ($J_{2,3}$ = 7.0 Hz) was in good agreement with puerin D ($J_{2,3}$–7.0 Hz) [15] indicating 2,3-*trans* axial relationship with a dihedral angle of 180°, (2*S*,3*R*) or (2*R*,3*S*) arrangement. To resolve this pair of enantiomer, the ECD spectrum of compound **1** was generated and the

Table 1
^{13}C (150 MHz) and ^{1}H (600 MHz) NMR Spectroscopic Data of Compounds **1–3** in CD_3OD.

Positions	**1**		**2**		**3**	
	δ_C	δ_H (*m*, *Hz*)	δ_C	δ_H (*m*, *Hz*)	δ_C	δ_H (*m*, *Hz*)
1						
2	82.7	4.66 d (7.0)	79.7	5.03 d (5.1)	78.1	4.85 d (9.2)
3	68.7	4.02 td (7.0, 4.9)	75.9	4.28 q (5.1)	72.2	3.88 dd (9.2, 3.6)
4	32.6	2.86 dd (15.7, 4.9) 2.69 dd (15.7, 7.6)	30.2	2.82 m 2.83 m	67.4	4.57 d (3.6)
5	131.3	6.87 d (8.2)	131.4	6.84 d (8.3)	132.4	7.15 d (8.3)
6	109.5	6.36 dd (8.2, 2.4)	109.5	6.36 dd (8.3, 2.4)	109.8	6.43 dd (8.3, 2.4)
7	158.0		157.9		160.0	–
8	103.6	6.32 d (2.4)	103.8	6.34 d (2.4)	103.3	6.29 d (2.4)
9	156.0		155.6		156.4	
10	112.4		112.3		115.8	
1′	136.8		136.7		136.2	
2′/6′	107.2	6.42 s	106.7	6.39 s	108.0	6.49 s
3′/5′	151.7		151.8		151.6	
4′	136.4		136.3		136.6	
4′-OCH_3	60.7	3.81 s	60.8	3.79 s	60.7	3.82 s
1″			103.6	4.31 d (7.7)		
2″			75.0	3.14 t (8.0)		
3″			78.0	3.30 m		
4″			71.5	3.25 m		
5″			77.8	3.25 m		
6″			62.7	3.88 dd (11.7, 1.9) 3.67 dd (11.7, 9.2)		

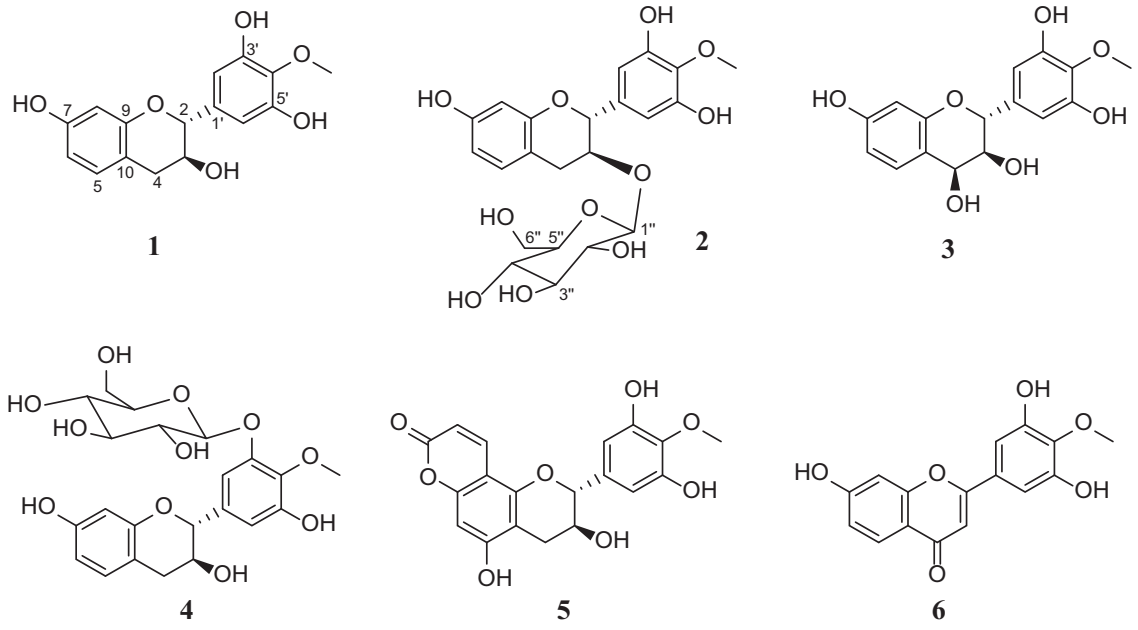

Fig. 1. Structures of compounds isolated from *Tetrapleura tetraptera*.

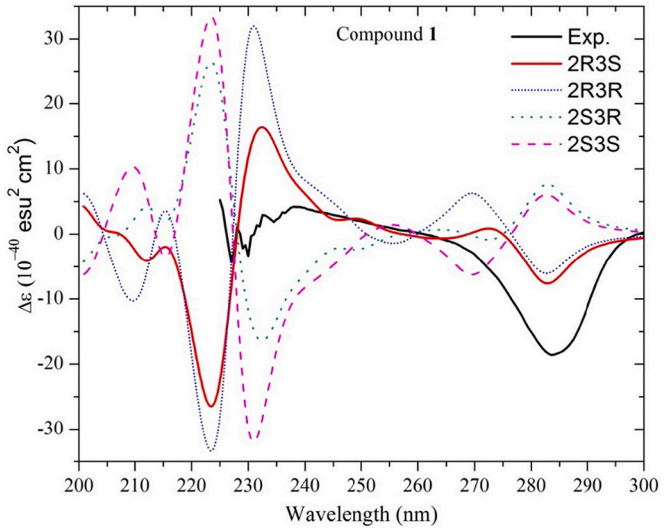

Fig. 2. Experimental and calculated electronic circular dichroism (ECD) spectra for compound **1** in methanol (*c* 0.3).

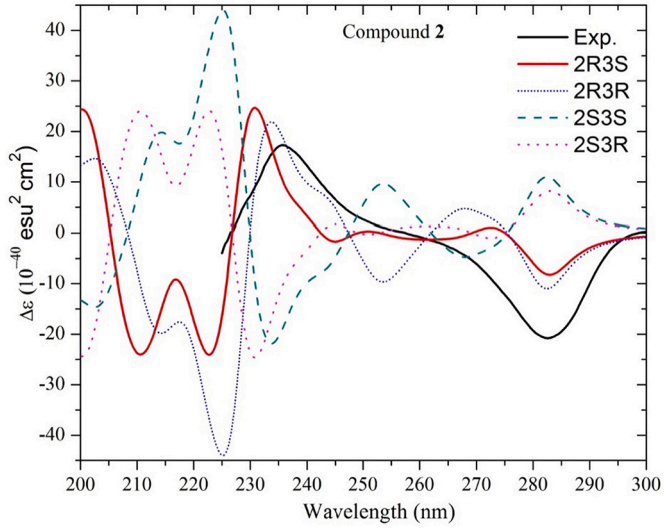

Fig. 3. Experimental and calculated electronic circular dichroism (ECD) spectra for compound **2** in Methanol (*c* 0.3).

results showed that **1** exhibited a negative Cotton effect around 280 nm indicating 2*R*,3*S* configuration [16]. The DFT calculated ECD spectrum of the structure with *2R,3S* configuration is a good agreement with the experimental spectrum. Based on all these data, compound **1** was identified as (2*R*,3*S*)-3,3′,5′,7-tetrahydroxy-4′-methoxyflavane.

Compound **2** was isolated as a white amorphous paste. The HRESIMS showed a peak at *m/z* 467.1554 $[M + H]^+$ (calcd for $C_{22}H_{27}O_{11}$, 467.1548) corresponding to the molecular formula $C_{22}H_{26}O_{11}$. The spectroscopic data of the aglycone moiety of compounds **1** and **2** were identical, indicating that this compound was a flavan-3-ol derivative as **1**. Comparison of its HRMS data with that of **1** showed a difference of 162 Da, which is equivalent to a hexose monosaccharide moiety. The ^1H NMR and the HSQC spectra revealed an anomeric signal at δ_H 4.31 (d, J = 7.7 Hz, H-1″ and δ_C 101.9, C1″) together with a set of signals between δ_H 3.14–4.31 in ^1H NMR and δ_C 62.7–78.0 in ^{13}C NMR, firmly established the presence of a β-D-glucopyranose [17]. The β- anomer was easily deduced from coupling constants values. Thus, the observed $J_{H1'',H2''}$ 7.7 Hz is typical value for a β- anomer, whereas the value for an α-anomer is generally less than 3.0 Hz [18]. Furthermore, analysis of the HRMS indicated fragment ion at *m/z* 305.1020 $[C_{16}H_{17}O_6]^+$ due to loss of glucose. An HMBC correlation between the anomeric proton δ_H 4.31 (H-1″) with carbon at δ_C 75.9 confirmed the position of the sugar moiety at C-3. Four stereoisomers (2*S*,3*S;* 2*R*,3*R;* 2*S*,3*R*; 2*R*,3*S*) were analyzed for **2**. By comparing the experimental and calculated ECD data, the (2*R*,3*S*) absolute configuration was suggested based on the negative Cotton effect (CE) observed at 280 nm (Fig. 3). Hence, the structure of **2** was unambiguously elucidated as (2*R*,3*S*)-3′,5′,7-trihydroxy-4′-methoxyflavane-3-*O*-β-D-glucopyranoside.

Compound **3** was isolated as a white amorphous paste with a molecular formula $C_{16}H_{16}O_7$, which was determined from HRESIMS at *m/z* 343.0786 $[M + Na]^+$ (calcd for $C_{16}H_{16}O_7Na$, 343.0788) and *m/z* 303.0863 $[M + H - H_2O]^+$ (calcd for $C_{16}H_{15}O_6$, 303.0863). Analysis of signals in the ^1H NMR spectra [(δ_H 4.85 (1H, d, J = 9.2 Hz, H-2), 3.88 (1H, dd, J = 9.2, 3.6 Hz, H-3), and 4.57 (1H, d, J = 3.6 Hz, H-4))] and ^{13}C [(δ_C 78.1 (C-2), 72.2 (C-3), and 67.4 (C-4))] indicated that compound **3** possess a flavan-3,4-diols skeleton [19–21]. The NMR spectra of compound **3** showed the same substitution pattern in A and B-rings as of compounds **1** and **2**. The notable difference being the presence of additional oxygen atom in the pyrone ring. This was further supported by HRMS which was 16 amu higher than **1**, indicating the presence of an additional oxygen atom in **3**. ^1H-^1H COSY correlation of H-2 with H-3 and H-3 with H-4 confirms the connectivity sequence in the C-ring. Furthermore, HMBC correlations observed from δ_H 4.57 (H-3) to δ_C 78.1 (C-2), and 72.2 (C-4). Likewise, the absolute configuration of **3** around the chiral centers was established using coupling constant observed between H-2 and H-3 in one hand and between H-3 and H-4 in the other hand. There are 8 possible stereoisomers (2*S*,3*S*,4*S*; 2*S*,3*S*,4*R*; 2*S*,3*R*,4*R*; 2*S*,3*R*,4*S*; 2*R*,3*R*,4*R*; 2*R*,3*R*,4*S*; 2*R*,3*S*,4*S*, and 2*R*,3*S*,4*R*). A preliminary analysis of the CD spectrum of compound **3**, displayed a slight negative cotton effect at 282 nm indicating a (2*R*) configuration. Further, a large ($J_{2,3}$ = 9.0 Hz) and small ($J_{3,4}$ = 3.6 Hz) coupling constants observed between signals for H-2/H-3 and H-4/H-3, respectively of the pyron ring (C-ring), implying the 2,3-*trans*-3,4-*cis* relative configurations [16]. The experimental ECD was also compared with the corresponding spectra of the 8 possible configurations (Fig. 4). Even though there is a baseline shift in the experimental spectrum, there is a good agreement with the calculated spectrum of the structure with the *2R,3S,4S* configuration. Thus, compound **3** was elucidated as (2*R*,3*S*,4*S*)-3,3′,4,5′,7-pentahydroxy-4′-methoxyflavane.

Since previous research work carried out in different part of *T. tetraptera* have showed considerable cytotoxicity against human cancer cell lines, the isolated compounds were tested for their

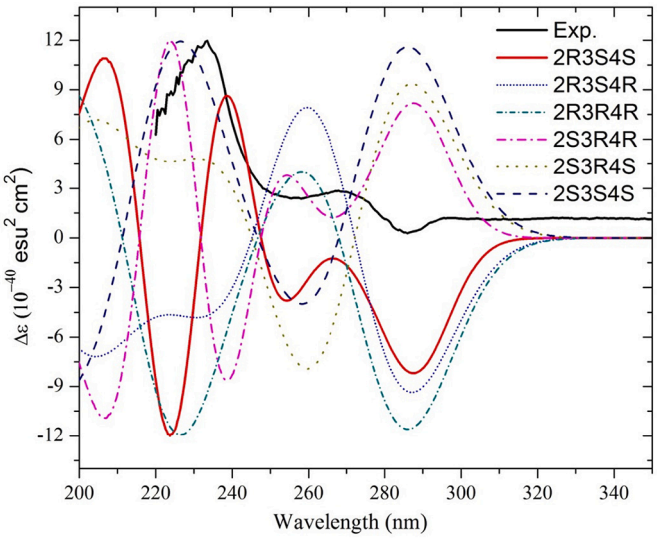

Fig. 4. Experimental and calculated electronic circular dichroism (ECD) spectra for compound **3** in Methanol (*c* 0.3).

cytotoxicity against leukemia cancer cell lines including drug-sensitive CCRF-CEM and its multidrug-resistant counterpart CEM/ADR5000 (Table 2). The tested compounds except **1** and **3** were not cytotoxic up to 100 μM. Compounds **1** and **3** demonstrates moderate activity against CCRF-CEM cell line with IC_{50} values of 21.90 and 35.10 μM, respectively. CEM/ADR5000 was sensitive towards compound **1** ($IC_{50} = 50.80$ μM), but resistant against **3** ($IC_{50} > 100$ μM), therefore it was considered as inactive.

3. Experimental

3.1. General experimental procedures

Reversed phase semi-preparative HPLC was performed on Shimadzu LC-20AP pump equipped with DGU-20A5R degassing unit, a Shimadzu SPD-M20A detector, a Shimadzu SIL-20ACHT auto-sampler and a Phenomenex Gemini C_{18} column (10 × 250 mm, 10 μm). Data were recorded and analyzed using LabSolutions software. For column chromatography, Silica gel 60 (0.063–0.2 mm, Macherey-Nagel) and Sephadex LH–20 (18–111 μm, GE Healthcare) were used as solid matrix. TLC was carried out on precoated silica gel 60 plates (0.20 mm). Compounds were visualized under UV light and further by spraying with H_2SO_4–EtOH (1:9, *v*/v). All solvents used were of analytical grade.

NMR experiments were recorded with a Bruker Avance III spectrometer operating at 600 and 150 MHz for ^1H and ^{13}C NMR, respectively. Spectra referencing were done using the residual solvent peaks. Specific rotation was recorded in Kruss Optronic Polarimeter P8000-T. ECD spectra was recorded on a Jasco J-715 spectrometer. IR analyses were recorded on a Bruker Tensor 27 FT-IR Spectrometer using a diffuse reflection apparatus. High-resolution electrospray ionization mass spectrometry (HRESIMS) was carried out on a LTQ Orbitrap spectrometer equipped with a HESI-II source.

3.2. Plant material

The stem bark of *Tetrapleura tetraptera* was collected from the University herbarium of the University of Ibadan, Nigeria. The plant was identified by Mr. Odenwo of the Herbarium of the Forestry Research Institute of Nigeria where voucher specimen (FHI 11041) was deposited.

3.3. Extraction and isolation

Pulverized stem bark of *T. tetraptera* (5.0 kg) was extracted thrice at ambient temperature using methanol (3 × 12 L, 72 h each) with constant agitation. The extract was filtered through filter paper and concentrated to dryness under vacuum to yield 520 g (10.4% yield) of dark brown residue. About 450 g of the extract was suspended in 400 mL of 20% aqueous methanol and was sequentially and exhaustively partitioned with *n* – hexane (5 L, 3 times), dichloromethane (5 L, 3 times), and ethyl acetate (5 L, 4 times). The partitioned fractions were concentrated to dryness under reduced pressure. The EtOAc fraction (110 g) was adsorbed with 200 g of florisil and chromatographically separated using silica gel as stationary phase and mixture of cyclohexane-EtOAc (9: 1, 8:2, and 1:1) followed by EtOAc-MeOH (10:0, 9:1, 8:2, and 7:3) as eluent affording seven fractions termed as $Fr_{1–7}$ which were pooled based on their TLC and LC–MS profiles.

Subfraction Fr_4 (1.19 g) eluted with pure EtOAc was further purified with semi-preparative HPLC using a gradient elution of 1:1 up to 10:0 of methanol in water (+ 0.1% formic acid) at a flow rate of 4 mL/min over 45 min to afford compounds **1** (4.2 mg, t_R 10.9 min), **2** (2.2 mg, t_R 10.2 min), **3** (1.1 mg, t_R 7.9 min), and **4** (0.9 mg, t_R 9.5 min). Purification of subfraction Fr_5 (2.6 g) obtained with EtOAc-MeOH (9:1 and 8:2) over silica column chromatography with EtOAc–MeOH (10:0, 9.5:0.5, 9:1, 8.5:1.5, 1:1, and 0:10) yielded 11 minor fractions labelled Fr_{5A-K} with different profiles on their LC – MS. Subfraction Fr_{5C} (694.4 mg) was further purified with semi-preparative HPLC using a gradient elution of 1:1 up to 10:0 of methanol in water (+ 0.1% formic acid) at a flow rate of 4 mL/min over 25 min to yield compounds **5** (0.8 mg, t_R 11.2 min), and **6** (1,4 mg, t_R 17.2 min).

3.4. Spectroscopic data

(2R,3S)-3,3′,5′,7-Tetrahydroxy-4′-methoxyflavane (**1**): Brown amorphous paste, LC-UV (MeOH-H_2O [+ 0.1% HCOOH]) λ_{max} 276 nm; $[\alpha]_D^{21}$ -1.739 (*c* 0.330, CH_3OH); IR (neat) ν_{max} 3354, 1623, 1600, 1509, 1458, 1355, 1155, 1037 cm^{-1}; ^1H and ^{13}C NMR data, see Table 1; HRESIMS *m/z* 305.1021 $[M + H]^+$ (calcd for $C_{16}H_{17}O_6$, 305.1019).

(2R,3S)-3′,5′,7-Trihydroxy-4′-methoxyflavane-3-O-β-D-glucopyranoside (**2**): Brown amorphous paste, LC-UV (MeOH-H_2O [+ 0.1% HCOOH]) λ_{max} 228 and 275 nm; $[\alpha]_D^{21}$ - 1.540 (*c* 0.330, CH_3OH); IR (neat) ν_{max} 3320, 1622, 1596, 1508, 1437, 1153, 1114, 1019 cm^{-1}; ^1H and ^{13}C NMR data, see Table 1; HRESIMS *m/z* 467.1554 $[M + H]^+$ (calcd for $C_{22}H_{27}O_{11}$, 467.1548).

(2R,3S,4S)-3,3′,4,5′,7-Pentahydroxy-4′-methoxyflavane (**3**): Brown amorphous paste, LC-UV (MeOH-H_2O [+ 0.1% HCOOH]) λ_{max} 277 nm; $[\alpha]_D^{21}$ 0.879 (*c* 0.330, CH_3OH); IR (neat) ν_{max} 3319, 1598, 1509, 1459, 1357, 1195, 1163, 1120, 1035 cm^{-1}; ^1H and ^{13}C NMR data, see Table 1; HRESIMS *m/z* 343.0786 $[M + Na]^+$ (calcd for $C_{16}H_{16}O_7Na$, 343.0788), *m/z* 303.0863 $[M + H – H_2O]^+$ (calcd for $C_{16}H_{15}O_6$, 303.0863).

3.5. DFT calculations

Density Functional Theory (DFT) and Time-Dependent Density Functional Theory (TD-DFT) calculations were performed using the B3LYP [12,13] functional together with Grimme's dispersion correction [22] and 6–311++G** [14] basis set. It has previously been demonstrated that this method is sufficient enough to describe the molecular geometries and spectroscopic analysis of related organic compounds [23]. To mimic the environment, the integral equation formalism polarizable continuum model (IEFPCM) [24] with methanol solvent parameters was employed for all the conformational analysis, geometry optimizations, and ECD calculations. Conformational analysis was performed for all the three compounds to identify the structures with the lowest energy on the potential energy surface. The optimized geometries were confirmed to be real minima on the potential energy surface with no imaginary frequencies by performing a normal-mode vibrational frequency analysis at the same level of theory. ECD calculations were performed at the same level of theory as the geometry optimizations. 250 states were taken for TD-DFT calculations. The calculated ECD wavelengths were scaled by a scaling factor of 1.08 for better comparisons with the corresponding experimental spectra. All the calculations were performed using the Gaussian program package (version G16-A.03) [25].

Table 2
Cytotoxicity of compounds **1–6**, and doxorubicin as determined by the resazurin reduction assay.

Compound	CCRF-CEM	CEM/ADR5000	Degree of resistance[a]
	IC_{50} in μM	IC_{50} in μM	
1	21.90 ± 0.60	50.80 ± 12.00	2.31
2	>100	>100	nd
3	35.10 ± 8.90	>100	>2.8
4	>100	>100	nd
5	>100	>100	nd
6	>100	>100	nd
Doxorubicin	0.0075 ± 0.0006	24.3 ± 1.8	3240

[a] The degree of resistance was calculated as the ratio of IC_{50} value in multidrug- resistant CEM/ADR5000 cells divided by the IC_{50} in sensitive CCRF-CEM cells. nd: not determined as no inhibitory concentration (IC_{50}) was observed up to 100 μM. Each experiment was performed thrice independently with every six replicates.

3.6. Cytotoxicity assays

Cell lines and cultures: Two leukemia cancer cell lines CCRF-CEM leukemia and CEM/ADR5000 were used. The cell lines were cultured under standard conditions (RPMI 1640 medium, 10% fetal calf serum, 1% penicillin/streptomycin; Invitrogen, Eggenstein, Germany) in an incubator (SteriCult, Thermo Fisher Scientific GmbH, Dreieich, Germany) at 37 °C and 5% CO_2. The multidrug resistance phenotype of the CEM/ADR5000 cells has been maintained by treatment with 5 μg/mL doxorubicin from 24 h every other week. The experiments were performed using cells in the logarithmic growth phase. The cell lines used in the current work, their origin, culturing, and resistance development were previously reported [26–28].

Resazurin reduction assay: The cytotoxic activity of compounds was evaluated using the resazurin reduction assay as described previously [29,30]. Cells were seeded in a density of 104 cells/well of 96 well plate and then treated with varying concentrations of compounds 1–6 (in DMSO), ranging from 10^{-5} - 100 μM. Briefly, resazurin is reduced to its highly fluorescent metabolite resorufin by living cells, whereas dead cells lack the property of converting resazurin. The fluorescent signals emitted by viable cells were detected by Infinite M2000 reader (Tecan, Grailsheim, Germany). Each experiment was performed thrice independently with every six replicates. IC_{50} values were calculated from dose-response curves using Microsoft excel.

CRediT author statement

Oguntimehin Samuel Ayoolu: Lab work, Writing, Draft preparation, Omonike Oluyemisi Ogbole: Supervision.
Edith Oriabure Ajaiyeoba: Conceptualization, Supervision.
Vaderament-A Nchiozem-Ngnitedem: Writing, Draft preparation, Data analysis.
Taye B. Demissie: DFT calculation, Software.
Mohamed Elbadawi: Bioassay, Data Analysis.
Thomas Efferth: Bioassay, Data analysis, Reviewing.
Kibrom Gebreheiwot Bedane: Supervision, Writing-Reviewing.
Michael Spiteller: Conceptualization, Supervision, Resources.

Declaration of Competing Interest

The authors declare no conflict of interest.

Acknowledgements

S.A.O. is grateful to the German Academic Exchange Service (DAAD) for a research grant at INFU, TU Dortmund. We are grateful for NMR analysis by Dr. Wolf Hiller (Faculty of Chemistry and Chemical Biology, TU Dortmund). We are thankful to Ms. Eva Wieczorek (INFU, TU Dortmund) for assistance with HRESIMS data acquisition. Computational resources were supplied by the project "e-Infrastruktura CZ" (e-INFRA CZ ID:90140) supported by the Ministry of Education, Youth, and Sports of the Czech Republic.

Appendix B. Supplementary material

The spectroscopic and spectrometric data of isolates (**1**–**3**) are available as supplementary material. Supplementary data to this article can be found online at https://doi.org/10.1016/j.fitote.2022.105206.

References

[1] S. Adesina, E. Iwalewa, I. Johnny, Tetrapleura tetraptera taub-ethnopharmacology, chemistry, medicinal and nutritional values- a review, Br. J. Pharm. Res. 12 (2016) 1–22, https://doi.org/10.9734/bjpr/2016/26554.
[2] H.J. Beentje, Kenya Trees, Shrubs, and Lianas, 6th edition, National Museums of Kenya, Nairobi, 1994, pp. 1–722.
[3] J.A.O. Ojewole, C.O. Adewunmi, Anti-inflammatory and hypoglycaemic effects of *Tetrapleura tetraptera* (Taub) [fabaceae] fruit aqueous extract in rats, J. Ethnopharmacol. 95 (2004) 177–182, https://doi.org/10.1016/j.jep.2004.06.026.
[4] A.T. Mbaveng, G.F. Chi, I.N. Bonsou, J.O. Ombito, S.O. Yeboah, V. Kuete, T. Efferth, Cytotoxic phytochemicals from the crude extract of *Tetrapleura tetraptera* fruits towards multi-factorial drug resistant cancer cells, J. Ethnopharmacol. 267 (2021), 113632, https://doi.org/10.1016/j.jep.2020.113632.
[5] V. Kuete, B. Krusche, M. Youns, I. Voukeng, A.G. Fankam, S. Tankeo, S. Lacmata, T. Efferth, Cytotoxicity of some Cameroonian spices and selected medicinal plant extracts, J. Ethnopharmacol. 134 (2011) 803–812, https://doi.org/10.1016/j.jep.2011.01.035.
[6] S.A. Fadeyi, O.O. Fadeyi, A.A. Adejumo, C. Okoro, E.L. Myles, In vitro anticancer screening of 24 locally used Nigerian medicinal plants, BMC Complement. Altern. Med. 13 (2013) 79, https://doi.org/10.1186/1472-6882-13-79.
[7] A. Aikins, P. Birikorang, M. Chama, E. Dotse, A. Anning, O. Appiah, Antiproliferative activities of methanolic extract and fractions of *Tetrapleura tetraptera* fruit, evidence-based complement, Altern. Med. 2021 (2021) 4051555, https://doi.org/10.1155/2021/4051555.
[8] R. Kusano, S. Ogawa, Y. Matsuo, T. Tanaka, Y. Yazaki, I. Kouno, α-Amylase and lipase inhibitory activity and structural characterization of acacia bark proanthocyanidins, J. Nat. Prod. 74 (2011) 119–128, https://doi.org/10.1021/np100372t.
[9] M. Fu, D. Deng, R. Huang, N. Zhang, Z. Su, S.X. Qiu, A new flavanocoumarin from the root of *Flemingia philippinensis*, Nat. Prod. Res. 27 (2013) 1237–1241, https://doi.org/10.1080/14786419.2012.724414.
[10] A.O. Oladimeji, O.A. Ibrahim, Mohammad AliS, Z. Ahmed, Flavonoids from the Roots of *Dioclea reflexa* (HOOK F.), Bull. Chem. Soc. Ethiop. 29 (2015) 441–448, https://doi.org/10.1055/s-0030-1271185.
[11] V.A. Nchiozem-Ngnitedem, L.K. Omosa, K.G. Bedane, S. Derese, M. Spiteller, Inhibition of proinflammatory cytokine release by flavones and flavanones from the leaves of *Dracaena steudneri*, Engl. Planta Med. 86 (2020) 1–9, https://doi.org/10.1055/a-1306-1368.
[12] P.J. Stephen, F.J. Devlin, C.F. Chabalowski, M.J. Frisch, Ab Initio calculation of vibrational absorption, J. Phys. Chem. 98 (1994) 11623–11627.
[13] D.B. Axel, Density-functional thermochemistry. III. The role of exact exchange, J. Chem. Phys. 98 (1993) 5648–5652.
[14] R. Krishnan, J.S. Binkley, R. Seeger, J.A. Pople, Self-consistent molecular orbital methods. XX. A basis set for correlated wave functions, J. Chem. Phys. 72 (1980) 650–654, https://doi.org/10.1063/1.438955.
[15] M.K. Tao, M. Xu, H.T. Zhu, R.R. Cheng, D. Wang, C.R. Yang, Y.J. Zhang, New phenylpropanoid-substituted flavan-3-ols from *Pu-er* ripe tea, Nat. Prod. Commun. 9 (2014) 1167–1170, https://doi.org/10.1177/1934578x1400900827.
[16] D. Slade, D. Ferreira, J.P.J. Marais, Circular dichroism, a powerful tool for the assessment of absolute configuration of flavonoids, Phytochemistry. 66 (2005) 2177–2215, https://doi.org/10.1016/j.phytochem.2005.02.002.
[17] J.M. Jin, Y.J. Zhang, H.Z. Li, C.R. Yang, Cytotoxic steroidal saponins from *Polygonatum zanlanscianense*, J. Nat. Prod. 67 (2004) 1992–1995, https://doi.org/10.1021/np049897u.
[18] M.U. Roslund, P. Tähtinen, M. Niemitz, R. Sjöholm, Complete assignments of the ^{1}H and ^{13}C chemical shifts and $J_{H,H}$ coupling constants in NMR spectra of D-glucopyranose and all D-glucopyranosyl-D-glucopyranosides, Carbohydr. Res. 343 (2008) 101–112, https://doi.org/10.1016/j.carres.2007.10.008.
[19] Y.B. Wu, Y.H. Kuo, M.A. Ouyang, Novel 4-(2-methylphenyl)-flavan, rhusjavanins A and B, from the roots of *Rhus semialata*, Nat. Prod. Res. 24 (2010) 1643–1647, https://doi.org/10.1080/14786419.2010.483528.
[20] A. Tchoukoua, T. Kuiate Tabopda, S. Uesugi, K. Kimura, E. Kwon, H. Momma, B. T. Ngadjui, T. Koseki, Y. Shiono, Two new 5-deoxyflavan-3,4-diol glucosides from roots of *Albizia chevalieri*, Magn. Reson. Chem. 54 (2016) 893–896, https://doi.org/10.1002/mrc.4504.
[21] Y.S. Bae, Flavan-3,4-diol Derivatives from the Heartwood of *Robinia pseudoacacia*, J. Korean Wood Sci. Technol. 29 (2001) 99–103.
[22] S. Grimme, Calculation of the electronic spectra of large molecules, Rev. Comput. Chem. 20 (2004) 153–218, https://doi.org/10.1002/0471678856.ch3.
[23] T.B. Demissie, M.S. Sundar, K. Thangavel, V. Andrushchenko, A.V. Bedekar, P. Bouř, Origins of optical activity in an oxo-helicene: experimental and computational studies, ACS Omega. 6 (2021) 2420–2428, https://doi.org/10.1021/acsomega.0c06079.
[24] J. Tomasi, B. Mennucci, R. Cammi, Quantum mechanical continuum solvation models, Chem. Rev. 105 (2005) 2999–3094, https://doi.org/10.1021/cr9904009.
[25] M.J. Frisch, G.W. Trucks, H.B. Schlegel, G.E. Scuseria, M.A. Robb, J.R. Cheeseman, J.A. Montgomery Jr., T. Vreven, K.N. Kudin, J.C. Burant, J.M. Millam, S.S. Lyengar, J. Tomasi, V. Barone, B. Mennucci, M. Cossi, G. Scalmani, R.E. Re, O. Yazyev, A. J. Austin, R. Cammi, C. Pomelli, J.W. Ochterski, P.Y. Ayala, K. Morokuma, G. A. Voth, P. Salvador, V.G. Dannenberg, J.J. Zakrzewski, S. Dapprich, A.D. Daniels, M.C. Strain, O. Farkas, D.K. Malick, A.D. Rabuck, K. Raghavachari, J.B. Foresman, J.V. Ortiz, Q. Cui, A.G. Baboul, S. Clifford, J. Cioslowski, B.B. Stefanov, G. Liu, A. Liashenko, P. Piskorz, I. Komaromi, R.L. Martin, D.J. Fox, T. Keith, M.A. Al-Laham, C.Y. Peng, M. Nanayakkara, A. Challacombe, P.M.W. Gill, B. Johnson, W. Chen, M.W. Wong, C. Gonzalez, J.A. Pople, Gaussian 16, Revision A., 03 ed, Gaussian, Inc., Wallingford CT, 2016.
[26] A. Kimmig, V. Gekeler, M. Neumann, G. Frese, R. Handgretinger, G. Kardos, H. Diddens, D. Niethammer, Susceptibility of multidrug-resistant human leukemia cell lines to human interleukin 2-activated killer cells, Cancer Res. 50 (1990) 6793–6799.

[27] T. Efferth, A. Sauerbrey, A. Olbrich, E. Gebhart, P. Rauch, H.O. Weber, J. G. Hengstler, M.E. Halatsch, M. Volm, K.D. Tew, D.D. Ross, J.O. Funk, Molecular modes of action of artesunate in tumor cell lines, Mol. Pharmacol. 64 (2003) 382–394, https://doi.org/10.1124/mol.64.2.382.

[28] V.-A. Nchiozem-Ngnitedem, L.K. Omosa, S. Derese, T. Efferth, M. Spiteller, Cytotoxic flavonoids from the seeds of *Dracaena steudneri* Engl against leukemia cancer cell lines, Phytomedicine Plus. 2 (2022), 100234.

[29] L.K. Omosa, V.A. Nchiozem-Ngnitedem, J. Mukavi, B. Atieno Okoko, H. Ombui Nyaboke, I. Hashim, J. Obegi Matundura, T. Efferth, M. Spiteller, Cytotoxic alkaloids from the root of *Zanthoxylum paracanthum* (mildbr) Kokwaro, Nat. Prod. Res. (2021), https://doi.org/10.1080/14786419.2021.1913586.

[30] K.G. Bedane, L. Brieger, C. Strohmann, E.-J. Seo, T. Efferth, M. Spiteller, Cytotoxic bufadienolides from the leaves of a medicinal plant *Melianthus comosus* collected in South Africa, Bioorg. Chem. 102 (2020), 104102, https://doi.org/10.1016/j.bioorg.2020.104102.